The evolution of a thermokarst-lake landscape: late Quaternary permafrost degradation and stabilization in interior Alaska

Mary Edwards*[1,2], Guido Grosse[3], Benjamin M. Jones[4], and Patricia McDowell[5]

[1]Geography and Environment, University of Southampton, Highfield, Southampton, SO17 1 BJ, UK; m.e.edwards@soton.ac.uk

[2]College of Natural Sciences and Mathematics, University of Alaska, Fairbanks, AK 99775, USA.

[3]Alfred Wegener Institute Helmholtz Centre for Polar and Marine Research, Telegrafenberg A45, 14473 Potsdam, Germany; guido.grosse@awi.de

[4]U.S. Geological Survey Alaska Science Center, 4210 University Drive, Anchorage, AK 99508, USA; bjones@usgs.gov

[5]Department of Geography, University of Oregon, Eugene, OR 97403, USA, pmcd@.uoregon.edu

*Corresponding author

ABSTRACT

Thermokarst processes characterize a variety of ice-rich permafrost terrains and often lead to lake formation. The long-term evolution of thermokarst landscapes and the stability and longevity of lakes depend upon climate, vegetation and ground conditions, including the volume of excess ground ice and its distribution. The current lake status of thermokarst-lake landscapes and their future trajectories under climate warming are better understood in the light of their long-term development. We studied lake-rich southern marginal upland of the Yukon Flats (northern interior Alaska) using dated lake-sediment cores, observations of river-cut exposures, and remotely-sensed data. The region features thick (up to 40 m) Quaternary deposits (mainly loess) that contain massive ground ice. Two of three studied lakes formed ~11,000-12,000 cal yr BP through inferred thermokarst processes, and fire may have played a role in initiating thermokarst development. From ~9000 cal yr BP, all lakes exhibited steady sedimentation, and pollen stratigraphies are consistent with regional patterns. Current lake expansion rates are low (0 to <7 cm yr^{-1} shoreline retreat) compared with other regions (~30 cm yr^{-1} or more). This thermokarst lake-rich region does not show evidence of extensive landscape lowering by lake drainage, nor of multiple lake generations within a basin. However, LiDAR images reveal linear “corrugations” (>5 m amplitude), deep thermo-erosional gullies, and features resembling lake drainage channels, suggesting highly dynamic surface processes have previously shaped the landscape. Evidently, widespread early Holocene permafrost degradation and thermokarst lake initiation were followed by lake

longevity and landscape stabilization, the latter possibly related to establishment of dense forest cover. Partial or complete drainage of three lakes in 2013 reveals there is some contemporary landscape dynamism. Holocene landscape evolution in the study area differs from that described from other thermokarst-affected regions; regional responses to future environmental change may be equally individualistic.

Key words: Alaska; Holocene; LiDAR; non-linear processes; permafrost degradation; thermokarst lakes.

1. **Introduction**

Thermokarst, the thaw of excess ice in permafrost-affected sediments that leads to ground collapse (French, 2007), is widespread in arctic and sub-arctic landscapes. Thermokarst (thaw) lakes form when water fills a basin caused by ground collapse. Thus, where unconsolidated surface material is underlain by permafrost and lakes are present, it is likely that thermokarst processes have played a role in lake formation and expansion. Recent field observations and detailed remotely sensed image time-series record current dynamism in many thermokarst lake regions (e.g., Smith et al., 2005; Jones et al. 2011; Lantz and Turner, 2015). Changes in the rate of current processes and/or the developmental direction of thermokarst lake landscapes (e.g., towards more or fewer lakes), should be expected as key drivers change. For example, climate warming is anticipated to enhance thermokarst activity in areas underlain by ice-rich permafrost. On the other hand, given permafrost degradation and/or precipitation-driven lake-level rise, lakes may drain via groundwater or surface overflow (Mackay 1988; Yoshikawa and Hinzman, 2003; Marsh et al., 2009; Grosse et al., 2013; Jones and Arp, 2015).

Key biogeochemical processes are associated with thermokarst lakes, such as release of CO_2 and/or CH_4 from microbial processing of organic materials within lakes and underlying sediments (Bastviken, 2004; Walter et al., 2006; Zulueta et al., 2011) or sequestration of carbon as peat in drained basins (Hinkel et al., 2003; Bockheim et al., 2004; Jones et al., 2012; Walter Anthony et al., 2014). Thermokarst lakes are possibly a substantial atmospheric methane

source (Walter et al., 2006, 2007 a, b). Consequently, they are a focus of interest in the Earth system science community. To understand past or future long-term contributions of thermokarst lakes to the northern carbon budget, we need to know how changes in key drivers might modify thermokarst processes. Local topography and hydrology interact to generate both increases and decreases in lake number and extent (Smith et al., 2005; Morgenstern et al., 2011; van Huissteden et al., 2011). Afforestation, peat development and vegetation mats encroaching on lakes reduce the tendency for thermokarst by increasing ground insulation (Jorgenson et al., 2010; Roach et al., 2011). Through modelling, Kessler et al. (2012) show that topography, lake developmental history and climate all play a role in determining the long-term evolution of lakes and thermokarst landscapes. Thus, any assumption of a steady state of lake formation and drainage, or of uniformity in thermokarst processes among regions, is unlikely to be realistic.

Furthermore, it may be that observed contemporary regimes of climate, permafrost, and vegetation are insufficient analogues for future responses to climate warming. A long-term perspective, however, can make use of past "natural experiments" to examine the impact of major past environmental change on thermokarst lake-rich landscapes. In this study we use field observations of Quaternary deposits, dated lake-sediment stratigraphies, and high-resolution remote sensing images and digital elevation data to investigate changes in late Quaternary thermokarst and landscape dynamics of a lake-rich upland bordering the Yukon Flats of interior Alaska (Fig. 1).

2. Thermokarst (thaw) lakes

Most northern lakes, including thermokarst lakes, are small, being <10 km in diameter (Arp and Jones, 2008; Paltan et al., 2015). Classic thermokarst lake forms include shallow (~2 m deep), often oriented lakes on the Arctic Coastal Plain of northern Alaska (Sellmann et al., 1975; Jorgenson and Shur, 2007; Arp et al., 2011). The spatial extent and drainage patterns of these lakes have been described by Hinkel et al. (2003, 2005, 2007). Deeper (~5 - >20 m) so-called *yedoma* thermokarst lakes are described by Zimov et al. (1997), West and Plug (2008), Walter et al. (2006), Morgenstern et al. (2011), Hinkel et al. (2012), and Fedorov et al. (2014). These occur in deep (usually > 10 m thick) Pleistocene deposits of ice-rich silt (*yedoma*; Schirrmeister et al., 2013), and are found, for example, in northeast Siberia and the northern Seward Peninsula of Alaska. Burn and Smith (1990), Burn (2002) and Lauriol et al. (2009) describe thermokarst lakes in northwest Canada. In many regions, numerous drained lake basins, often with several generations superimposed, indicate episodic or continual lake formation and drainage over centuries to millennia (Hinkel et al., 2003; Jones et al., 2012; Jones and Arp, 2015).

Stratigraphic studies that observe lake development over long time periods provide a valuable perspective on thermokarst processes. For example, on a regional scale, observations of numerous lake profiles in natural exposures in Siberia and northwest North America indicate that thermokarst activity and lake initiation was focused on the early Holocene (ca 11,000-9,000 yr BP;

summarized in Walter et al., 2007a), whereas in northeast Siberia drainage and infilling of lake basins has become an important process in the late Holocene (Walter Anthony et al., 2014). At the local scale, detailed studies of individual lakes provide insight into how those lakes developed over time, e.g., Murton's (1996) study of exposed thermokarst-lake sediments in the western Canadian Arctic. Rapid changes in sediment characteristics with depth often indicate highly dynamic lake paleoenvironments (Lenz et al., 2015; Farquharson et al., accepted).

3. Study Area

The Yukon Flats comprise a broad structural basin bordered by low uplands in northeast interior Alaska. The area lies in the boreal forest zone just south of the Arctic Circle (Fig. 1). It experiences a cold continental climate (January mean, -28°C; July mean, +17°) and annual precipitation of ~150-200 mm (much falling as rain in summer and early autumn). Spruce-dominated forest (*Picea glauca* and *P. mariana*) is the zonal vegetation type, with seral stands of aspen (*Populus tremuloides*) and birch (*Betula neoalaskana*) after fire, the most common large-scale disturbance (Kasischke et al., 2010). The forest ascends to about 900 m asl in the mountains to the south.

Williams (1962) described the Quaternary geology of the Yukon Flats. The Yukon River traverses the flat, central alluvial lowland at about 150 m asl. The uplands rise up to 100 m above the floodplain. The southern marginal upland is a high-level terrace formed of alluvial gravels capped by Pleistocene loess up to 35

147 m thick. It has subdued but rolling topography. Aerial observations show linear
148 ridges and swales trending NE-SW in the west and more complex surface
149 features muted by dense forest cover in the central and eastern areas (Figs. 2
150 and 3). Northward-flowing tributaries of the Yukon River cut through the upland,
151 exposing river-cut sections in places.

152

153 ***3.1 Late Quaternary history***

154 The late Quaternary environmental and climate history of interior Alaska featured
155 dramatic changes, particularly in moisture levels. The region remained ice-free
156 during the last glacial period. Prior to ~14,000 cal yr BP, conditions were cooler
157 overall (Bartlein et al., 1991, 2014) and far drier than present, with precipitation
158 possibly 50% of modern values (Barber and Finney, 2000). Non-woody
159 vegetation dominated, with shrubs likely confined to sheltered drainages. A
160 change to moister conditions ~13,000 cal yr BP was manifest in lake-level
161 increases (Barber and Finney, 2000) and a shift from herb-dominated to woody
162 vegetation (Anderson et al., 2004). These changes were linked to a major
163 deglacial shift in hemispheric circulation that replaced a large-scale anticyclone
164 centered on the Laurentide ice sheet with a westerly airflow across Alaska
165 (Bartlein et al., 1991, 2014). *Betula* expanded, as evidenced by a pollen increase
166 from a few percent to values of >50%. Between ~12,000 and 10,000 cal yr BP
167 *Populus* characterized vegetation at many sites (Anderson et al., 2004). During
168 this time, summers were warmer (and winters cooler) than present (Kaufman et
169 al., 2004; Bartlein et al., 2014). Through the Holocene the interior Alaskan

climate has gradually become less seasonal. Lake levels rose further at about 10,000 cal yr BP (Abbott et al., 2000), coincident with an expansion of *Picea*, then *Alnus* (alder), signaling the regional establishment of conifer-dominated forest.

3.2 Study lakes

Both the central lowland and the marginal upland are characterized by numerous lakes with a range of morphologies. Here we discuss only the lakes of the marginal upland (for studies of lakes in the Yukon Flats lowland see Heglund and Jones, 2003; Walvoord et al., 2012; Jepsen et al., 2013). The upland lakes have received relatively little attention (but see Williams and Yeend, 1979). Edwards and Hopkins (1988) identified three lake types (Fig. 2): i) lakes that occur in swales (swale lakes); ii) lakes that indent high ground, typically have no outlet, and are roughly isodiametric (perched lakes); and iii) lakes occupying valleys with underfit streams (i.e., streams smaller than would be suggested by their valley size), sometimes in strings, and typically elongate (valley lakes).

Three lakes in the upland region were surveyed and cored in the 1980s and 1990s: Sands of Time Lake (SOT, 66.030° N, 147.548° W), Six-Loon Lake (6LL, 66.119° N, 145.845° W), Dune-2 Lake (D2, 66.058° N, 145.789° W); all names are informal. The study lakes represent the three main types of lake described above. Sands of Time Lake (SOT – Figs. 1, 2a) lies in a swale between NE-SW trending ridges. It is about 2.0 km in length. Its elongate shape and location may be related to the ridge-swale topography, the origin of which is unknown. Steep

loess bluffs, 5-10 m high and stabilized by grassy vegetation, form parts of the shoreline. The lake is shallow around the edges and features a prominent near-shore ledge, probably formed from prograded sediment eroded from the bluffs. It deepens outward to a depth of about 10 m.

Six-loon Lake (Figs. 1, 2b) is a perched lake. The 6LL surface lies several meters below the surrounding land surface. Shallow water close to shore deepens rapidly outward, and the central portion of the lake bed slopes gently to a maximum depth of ~13 m, creating a tank-shaped bathymetry. In an exposure on the isthmus separating 6LL from the adjacent lake to the west we observed shelly deposits resembling current shoreline material ~2 m below the surface and about 11 m above current lake level. Dune 2 Lake (Figs. 1, 2b) is a large, deep lake, one of a string lying in a valley in the central portion of the study area. D2 has multiple basins that are between 12 and 20 m deep and separated by underwater ridges.

4. Methods

4.1 Field survey

We surveyed the region via aerial observation and helicopter landings and by floating northward-flowing tributaries of the Yukon River in the 1980s and 1990s (Fig. 1). Dense forest cover meant few points were accessible except along river courses and lake shores. We described exposed sections of unconsolidated

214 sediments, observed meso-scale landscape features, and noted the occurrence
215 and form of ground ice in deposits.

216

217 ***4.2 Remotely Sensed Data***

218 We used historical color infrared photography from 1978 and contemporary high-
219 resolution Ikonos satellite imagery from 2009 to examine lake expansion rates at
220 eight lakes in the study area that we classified as perched lakes: embedded in
221 higher ground with no inflow. The spatial resolution of the geo-registered
222 imagery was 1 m. Lake shorelines were digitized manually in the remotely
223 sensed imagery and their perimeters analyzed using the USGS digital shoreline
224 analysis tool (http://woodshole.er.usgs.gov/project-pages/DSAS/) to determine
225 lake expansion or contraction rates (following the methods described in Jones et
226 al., 2011). Changes in the lake perimeter were sampled at 50 m increments for
227 all eight lakes.

228 We also examined a high-resolution (2 m grid cells) bare-earth digital
229 terrain model derived from airborne Light Detection and Ranging (LiDAR) data
230 acquired between 14 July and 03 September 2009 by the U.S. Geological Survey
231 (http://earthexplorer.usgs.gov) that reveal previously unobserved details of the
232 surface geomorphology. Terrain and landform elevation profiles derived from the
233 digital terrain model were also created across portions of the marginal upland to
234 determine their relief relative to modern-day lake surface elevations. In addition,
235 we used two Landsat ETM+ scenes to assess the catastrophic drainage of three
236 lakes in the study area during the summer of 2013.

4.3 Stratigraphic records from lakes

Low-resolution bathymetric transects were carried out via float plane or dinghy, using compass coordinates. Lakes were cored in summer over open water from an anchored raft using a modified piston corer (Wright, 1967). Cores were extruded on site, wrapped in plastic film and foil and returned to the lab, where they were stored at ~4°C. Lithology was described, organic content estimated by percent weight-loss on ignition (SOT, 6LL), and pollen samples processed using conventional techniques and counted to a sum of at least 300 terrestrial grains (Faegri and Iversen, 1989). Pollen data were visualized using TILIA software written by E. Grimm. Conventional radiocarbon dating on bulk sediment samples (material was collected and dated prior to the advent of AMS techniques) was carried out by Beta Analytic Inc. Abrupt changes and likely unconformities in the stratigraphies at 6LL and D2 (see below) meant we did not construct age models; instead, individual dates were converted to median calibrated ages using OxCal (https://c14.arch.ox.ac.uk) based on IntCal 13 (Reimer et al., 2013).

5. Results

5.1 Stratigraphy of the southern marginal upland

The presence of Quaternary tephra layers and the results of thermoluminescence dating at Birch Creek (Fig. 1) confirm the Quaternary age of the deposits (Edwards and McDowell, 1991; McDowell and Edwards, 2001;

259 Bigelow et al., 2014). Where the Yukon tributaries (hereafter called creeks) and
260 lake margins cut into the upland, we observed thick (10-40 m) exposed bluffs
261 composed predominantly of silt. The silt units varied in character. We identified
262 homogeneous and virtually structureless silt as airfall or retransported loess.
263 These inorganic silt units had loss-on-ignition values typically <3% and were up
264 to 15 m thick. We assumed silt that was strongly laminated and contained peaty
265 or woody organic debris layers to be retransported loess. The retransported
266 loess, where present, formed the uppermost unit below modern forest soil and
267 the unit varied in height from ~2-6 m. Along the creeks the silt-dominated
268 sediments were underlain at varying heights above river level by fluvial sand
269 and/or fluvial gravel/cobbles, sometimes with inclusions of organic debris (see
270 supplementary material for further details).

271 Silt and sand units, while frozen inward from the exposed surface, had
272 little interstitial ice. However, large (>5 m deep) syngenetic ice wedges were
273 present throughout the area (Fig. 4). Where observed, these varied in height
274 below the modern surface. At Birch Creek, Edwards and McDowell (2001)
275 observed large, flat-topped ice bodies ~2 m below the modern surface in loess
276 and ~25 m below the surface in a loess/palaeosol unit that dates to MIS 6 or MIS
277 5. At Beaver Creek a large ice-wedge pseudomorph occurred at ~15 m below the
278 surface; the large ice body ice shown in Fig. 4 is also ~15 m below the surface,
279 but its upper limit is obscured. Visible ice wedges tended to be widely spaced
280 compared, for example, with the abundance of observable wedges in the Kolyma
281 lowland (Murton et al., 2015) or North Slope foothills of the Brooks Range

(Kanevskiy et al., 2011). Ice bodies exposed near valley bottoms were variable in shape and may represent segregation ice masses in relatively moist creek floodplains. While ice-wedge polygons attributable to epigenetic wedges are visible from the air, exposures only occasionally revealed ice <2 m below the surface.

5.2 Surface landforms

Several types of landform recognized from aerial observations (Fig. 3) are clarified in the LiDAR elevation data (Fig. 5). Gullies, apparently cut by water, occur along the northern escarpment of the marginal upland or end in lakes (Fig. 5a). Drainage channels emerging from lakes (Fig. 5a-d and see also Fig. 3), and numerous other channels and shallow seeps, are apparently water-eroded, but many no longer have perennial streams, particularly in the central and eastern parts of the study area. “Corrugations” often, but not always, occur sub-parallel to the slope with a wavelength of ~75-100 m and a swale-ridge height of ~5 m. Some also occur perpendicular to the slope, appearing as regularly spaced parallel gullies. Corrugations are often interrupted by lakes. Where we were able to view corrugations in cross section in the field, they were formed of homogeneous silt (Fig. 5b,c).

Aerial images and LiDAR data show lakes with shorelines well below the surrounding land surface (Fig. 5 a-c). Lakes of different surface heights are interconnected by apparently inactive deep drainage channels (Fig. 5d). In Fig. 5c the measured lake surface lies ~10 m below the surrounding upland. Many lakes appear to have partially drained via now inactive channels. At several lakes

we visited, we observed shelly deposits typical of shallow, nearshore locations above the current shoreline (e.g., 6LL, see section 3.2), which provide further circumstantial evidence in support of lake-level dynamism.

5.3 Contemporary lake processes

The comparison of georeferenced images for eight perched lakes indicated that most lake bluff lines remained stable during the 31-yr period between image acquisitions. Mean bluff erosion ranged from non-detectable to <7 cm yr^{-1}. While expansion through time is unlikely to have been linear, the mean can usefully be compared with mean values calculated for other regions.

In June 2013, three lakes catastrophically drained: one perched lake drained completely, another drained partially, and one valley lake drained partially. Comparison of Landsat ETM+ imagery acquired in July 2012 and August 2013 shows the effect of lake drainages: freshly exposed sediment is visible along the lake margins as well as along the drainage pathways. In addition, well developed sediment fans are visible in the down-drainage direction (Fig. 6). The fans confirm that lateral drainage was the dominant cause of the lake-level changes observed at these three sites, rather than lowering via evaporation or internal drainage through a talik.

Forest fires are common across interior Alaska and burned areas were also prominent on our aerial traverses of the marginal upland. A fire burned part of the catchment of SOT in 1988 (see Fig. 2a). The removal by fire of vegetation

and organic soil from the ground surface can lead to the mobilization of exposed silt, even on gentle slopes, as shown by flows of silt, some of which reach lake margins (ME, pers. observation, 1992; L. Anderson, pers. communication, 2015). Increased influx to the lake created a new silt shelf at the shoreline. We observed no direct evidence that fires have initiated new thermokarst lakes or lake drainage. However, the forest surrounding the three documented lake drainage events did burn recently (2009; Fig. 6).

5.4 Lake sediment chronology, lithology and biostratigraphy

Radiocarbon details for the lakes are given in Table 1. No dates were discarded.

At SOT, there are no sharp transitions in the sediment record. Full-glacial sediments are sandy silt grading upwards to silt, with another gradual transition to more organic silt dated around 10,000 ^{14}C yr BP (Fig. 7a). Occasional inorganic laminae, visually distinguishable by their paler color, predominantly composed of silt (by microscopic inspection), and up to 1 cm thick occur in this more organic sediment.

In contrast, at 6LL (Fig. 7b), a 380-cm core from the lake center contains inorganic silt at the base (with a date of 21,841±359 cal yr BP on bulk sediment), but at 310 cm there is an abrupt transition to almost 1 m of intermixed peat, silt, and shell-rich layers, with abundant charcoal. This horizon accumulated between ~ 12,500-10,500 cal yr BP. At about 170 cm the sediments grade into more organic silt, then to silty gyttja with some fine laminations. Freshwater shells typical of nearshore deposits are present at ~50 cm depth. The available radiocarbon dates suggest these probably accumulated 5000-4000 cal yr BP. No

data are available for the uppermost 30 cm of the core, as watery sediment was lost on extrusion. Variable loss-on-ignition values reflect the mixture of silt and organic detritus between 310 and 170 cm depth but are generally <15%. They increase to mostly >30% in the overlying lake sediments, but values drop to 10-15% at 80-30 cm depth.

D2 was cored on the lower slope of one of its basins (~14 m deep). The 650 cm-long core has inorganic silt at the base. From 580-390 cm silt layers are interbedded with layers of woody and herbaceous detritus or peat (Fig. 8C). The three lowermost radiocarbon dates show reversals and overlaps over the period ~13,500-12,000 cal yr BP, suggesting the detrital layers and intervening silt were deposited rapidly and possibly chaotically. Above 390 cm is organic silt that contains visually distinct pale inorganic laminae up to 1 cm thick (see SOT above). Above 80 cm is homogeneous silty gyttja.

In the pollen record at SOT (Fig. 7a), the *Populus* subzone ~13,000-10,000 yr BP and the increases in *Picea* and *Alnus* at ~10,000 and 9000 cal yr BP, respectively, match the regional pollen stratigraphy (see section 2). However, the *Betula* rise is dated at ~20,000 cal yr BP and is clearly too old; we discuss the probable reasons for this below. The 6LL and D2 records (Fig. 8b,c) broadly conform to the regional pattern. The *Betula* rise (~13,000 cal yr BP) is followed by a *Populus* period between ~12,000 and 10,000 cal yr BP, then by *Picea* and *Alnus* rises. At D2, these latter two events are dated slightly earlier than the regional norm (considered to be ~10,000 and 8500~ cal yr BP, respectively; see section 2). However, the early ages are probably an artefact, as

373 both pollen and dating are likely affected by the initial rapid and chaotic
374 sedimentation at the coring location.

375

376 **6. Discussion**

377 The combined approaches of field observations, remote sensing, and lake-
378 sediment analyses allow us to construct a developmental model for the southern
379 marginal upland landscape of the Yukon Flats during the late Quaternary (Fig. 8).
380 This includes the formation and development of the lakes within the landscape,
381 the likely long-term drivers of landscape change, and possible reasons for
382 differences from other regions.

383

384 ***6.1 Late Quaternary landscape dynamics and lake formation***

385 Both our field observations and those of Williams (1962) confirm a surficial
386 geology susceptible to thermokarst: a thick cover of Quaternary silt and sand,
387 largely derived from aeolian deposition (but fluvial near current river level) and
388 widely distributed massive ground ice in the form of large ice wedges.
389 Furthermore, studies at Birch Creek (BC-1, see Fig. 1) report Pleistocene-aged
390 paleosols, ice-wedge casts, and pond sediments related to an ancient beaver
391 dam, which suggests landscape dynamism has been a persistent feature of this
392 region during the Quaternary (Edwards and McDowell, 1991; McDowell and
393 Edwards, 2001; Bigelow et al., 2014).

While landscapes may be dramatically transformed by lake formation, other geomorphic processes related to permafrost degradation may also shape the landscape and interact with the dynamics of lake formation. Edwards et al. (1995) conjectured that non-lacustrine, mesoscale landforms in the densely forested Alaskan interior, including the study area, were likely related to thermokarst processes. However, such landforms are notoriously difficult to investigate in densely forested terrain. The LiDAR imagery used here exposes the detailed surface features of the marginal upland, showing that past permafrost degradation has dramatically transformed the whole landscape.

The unusual land-surface features revealed by the LiDAR elevation data suggest that at some time in the past, soil and sediment were highly mobile. Surface corrugations with amplitudes sometimes exceeding5 m run parallel to the slope, suggesting multiple slope failures and downward slippage, or they run perpendicular to the slope, reflecting drainage and sediment removal. Both features suggest that surface silt was transported to lower areas. Lakes intersect these surface features and thus the corrugations must be older than lakes. If most lakes originated in the early Holocene (see below), the surface features are at least this age, or older.

Drainage channels cut into the upland margin, run downslope into lakes, and leave lakes (Fig. 5A). This implies further transport and deposition of sediment via channelized water movement. While the landscape clearly became stabilized, as indicated by the preservation of the surface topography and lakes, lake drainages have likely occurred throughout the Holocene. Several drainage

events observed in 2013 confirm that some landscape readjustments are still occurring. Given the evident dynamism of the landscape, it is interesting that the majority of lakes have remained undrained or only partially drained (e.g., the ~10 m lowering observed in Fig 5c). There is no evidence of multiple generations of lakes similar to that observed in many coastal lowlands of northern and western Alaska, Siberia, and Canada (Hinkel et al. 2005; Jones et al., 2011; Grosse et al., 2013). We conclude that the formation, dramatic lowering, and subsequent stabilization of lakes were mostly, but not entirely, late glacial/early Holocene in age.

Twentieth-century erosion of lateral lake shorelines has been low (mean: 7 cm yr^{-1}) compared with lakes on the northern Seward Peninsula (mean of up to 39 cm yr^{-1}; Jones et al., 2011) or the Arctic Coastal Plain of northern Alaska (landscape-scale rates of 180 cm yr^{-1}; Arp et al, 2011). In these other regions, lakes typically are breached or drain a few thousand years after formation (Hinkel et al., 2003; Farquharson et al., accepted), and thus lakes originating in the Pleistocene or earliest Holocene have mostly already drained. This is also the case in northeast Siberia, where numerous riverbank exposures reveal thaw-lake sediments dating to the first part of the Holocene overlain by peat and the modern land surface (summarized in Walter et al., 2007b). In contrast, in our study area, all studied lakes are at least 10,000 years old.

6.2 Modes of lake formation

439 The studied lakes do not all have the same origin. SOT formed in a swale and
440 conforms to Jorgenson and Shur's (2007) description of a lake that, while in a
441 permafrost-affected landscape, occupies a pre-existing basin. Possibly, the
442 ridges are ancient linear sand dunes mantled with silt, although sand was rare in
443 the sediment core and nearby river-cut sections.

444 Sedimentation occurred in the basin during the LGM, when the site was
445 either a shallow pond or perhaps an intermittently flooded seepage, given the
446 occurrence of aquatic pollen and *Salix* wood in the basal sediment.
447 Sedimentation was predominantly of silt between ~22,000 and 13,000 yr BP.
448 However, high (50%) amounts of *Betula* pollen between 18,000 and 14,000 cal yr
449 BP occur far too early, based on the regional stratigraphy. A similar mismatch of
450 chronology and biostratigraphy was recorded at Antifreeze Pond, Yukon, a kettle
451 lake in glacial till (Rampton, 1971). In both cases, bulk sediment was dated. AMS
452 dates on new material from Antifreeze Pond, place the *Betula* rise consistent with
453 regional pollen records (Vermaire, 2005). Possibly, during the *Betula* zone at
454 SOT, large amounts of older, allochthonous material containing silt and some
455 organics were introduced into what was already a shallow lake basin, where they
456 mixed with recently deposited organic material and pollen. Under the warmer and
457 moister deglacial climate, with deeper thaw and greater runoff, and with a still
458 unstable land surface, the highly mobile silt would have readily moved downslope
459 and into the lake.

460 In contrast, both 6LL and D2 have basal sediments of inorganic silt
461 overlain by thick (>10 cm) inorganic silt layers alternating with organic, shallow-

462 water sediments containing terrestrial plant material, aquatic molluscs, and
463 charcoal. These sediment packages are too deep to represent the untransformed
464 permafrost-affected active layer. They rather resemble the "trash layer"
465 described from the base of thaw lakes, caused as the soil and vegetation
466 collapsed over melting ice (Hopkins and Kidd, 1988; Farquharson et al.,
467 accepted). Pollen of *Typha* (D2) and freshwater mollusk shells indicate shallow-
468 water conditions at this time. If the initial ponds were shallow, sediment freezing
469 and potential cryoturbation after the pond froze to the bottom could have further
470 contributed to the chaotic nature of the sediments. Basin formation dates to the
471 late glacial period and Holocene transition (~13,000-11,000 cal yr BP), the period
472 reported more broadly across Alaska and Siberia as one of widespread
473 thermokarst lake formation (Walter et al., 2007b).

474 High silt content and/or intermittent-to-common silt laminae in early- to
475 mid-Holocene sediments in all records indicate continued input of terrestrial
476 material, but sediments deposited later in the Holocene generally have a greater
477 proportion of fine, autochthonous material (at 6LL, organic content reaches
478 >30%). The lake sediment records suggest progressive change due to: i)
479 considerable slope movement and/or thermokarst, ii) lake deepening and
480 expansion, and/or iii) stabilization of lake catchments. At 6LL, shell-rich layers in
481 the upper sediments suggest shallow water or shoreline conditions 4000-5000
482 years ago, after the lake initially deepened and sedimentation stabilized. The
483 relict drainage intersecting the lake may, therefore, be a Holocene overflow
484 channel that resulted in lake lowering, a possible modern analogue being the

observed 2013 drainage events. It is possible that the narrow and deep drainage channels are prone to collapse and allow the re-damming of a lake after partial drainage events. The observed mobility of the silt supports this conjecture.

6.3 Drivers of change

Disturbances to the ground thermal regime in ice-rich permafrost landscapes are required to initiate thermokarst. For thermokarst to become widespread, climate—in particular water balance—must be favorable. From the lacustrine sediment record, we conclude that the main thermokarst period in the study area dates to ~13,000-10,500 cal yr BP. This is coincident with a change from dry to moister conditions, manifest in lake-level increases in interior Alaska, plus late glacial warming (Abbott et al., 2000; Barber and Finney, 2000; Bartlein et al., 2014). These changes are associated with widespread thermokarst lake initiation in northwest North America and Siberia (Walter et al., 2007a). Around 5000-3000 cal yr BP, the regional water balance probably reached its most positive Holocene state (Abbott et al., 2000), and greater precipitation may have increased run off and lake levels. Interestingly, this coincides with the possible partial drainage of 6LL. Today, the region is characterized by low precipitation and often features a summer water deficit (Riordan et al., 2006). Shallow lakes in the Yukon Flats lowlands have shrunk or even disappeared due to evaporative losses exceeding water supply (Anderson et al., 2013). Such conditions may maintain lakes in the marginal upland well below their sills, thus reducing the chance of overflow and drainage due to down-cutting.

Vegetation cover influences soil stability and permafrost dynamics (Jorgensen et al., 2010). Prior to the late glacial climate shift at ~13,000 yr BP, conditions were arid, woody growth forms rare and the vegetation cover likely incomplete (Anderson et al., 2004). The silt-covered surface would have been open to eolian erosion and transport and, possibly, degradation of ice-rich sub-surface deposits. As the climate became wetter, the surface would have been increasingly mobilized by precipitation events and snow melt. While expansion of woody vegetation cover potentially provided greater stabilization of surface sediment, the occurrence of fire in the warm, dry early-Holocene summer season, as evidenced by charcoal in the trash-layer deposits at 6LL and D2, suggests an increasing probability of disturbance-mediated thermokarst in the early Holocene. Fire-induced thermokarst development has also been inferred from charcoal layers in thermokarst lake sediment cores from central Yakutia (Katamura et al., 2009).

Under contemporary seral stands of *Betula* or *Populus* on well-drained surfaces there is usually little in the way of an insulating moss mat or an organic litter layer and far less shade than under a spruce canopy. Such conditions allow downward heat penetration and maintain a deep active layer when permafrost is present (Viereck, 1970). Such conditions would have been common in the early Holocene, but with the expansion of *Picea* in the region 10,000 yr BP, surface conditions would have changed. The increase in *Picea* pollen is accompanied by increases in *Sphagnum* spores and ericaceous shrub pollen. These indicate the establishment of moss-heath ground cover, which is associated with thick,

531 insulating, organic-rich soils of the type widespread in today's boreal forest. By
532 the mid-Holocene, spruce forest was dominant. While there is evidence of
533 continued burning from regional charcoal records (e.g., Kelly et al., 2013), the
534 main influence of spruce forest on the marginal upland is likely to have been to
535 diminish active-layer thickness, stabilize soil temperatures and reduce sediment
536 mobility, as suggested by Jorgensen et al. (2010) for other interior regions.

537 The early Holocene spread of *Populus* and *Salix* may have led to
538 population increases in beavers. Robinson et al. (2007) report stratigraphic
539 evidence of early-Holocene beaver ponds near the Yukon River, and an
540 interglacial-age beaver-dammed pond occurs in the BC-1 section (Edwards and
541 McDowell, 1991). It is not inconceivable that beaver activity may have initiated
542 the formation of some ponds particularly along drainages.

543 The evolution of thermokarst strongly depends on ground-ice conditions.
544 Our observations and those of Williams (1962) suggest that the syngenetic ice
545 wedges in the sediments draping the southern marginal upland have a
546 heterogeneous distribution and are sparse compared with other areas in Alaska
547 (e.g., Seward Peninsula, Hopkins and Kidd, 1988; and the North Slope of the
548 Brooks range, Kanevskiy et al., 2011). This may be a result of dry conditions
549 during their formation. Furthermore, the tops of the wedges are typically several
550 meters below the present land surface. For any ice forming in the last glacial
551 cycle, deep wedge tops may be the consequence either of burial with aeolian
552 sediment during drier periods or deep surface thaw during deglaciation. In
553 northeast Siberia, a "transition layer", often >1 m thick and identifiable by thin,

554 sub-horizontal ice lenses (see Murton et al., 2015) overlying syngenetic wedge
555 tops, represents material that first thawed, then re-froze, in the Holocene. A
556 similar feature has been described in northwest Canada (Burn, 1997). While no
557 fine ice structure is observable in the permafrost of the marginal upland, the
558 larger-scale disruption of the land surface may be a different expression of early-
559 Holocene deep thaw. The greater depth and sparser network of the ground ice
560 may limit thermokarst activity today; whether it affected past processes we
561 cannot say, but it seems probable that at least some ice loss is the result of the
562 deglacial events recorded in the marginal upland landscape.

563

564 ***6.4 Synthesis: evolution of thaw-lake landscapes, past, present and future***

565 The silt-covered terrain of the marginal upland, which is underlain by permafrost
566 that features massive ice, experienced widespread, rapid thermokarst
567 development with the onset of late glacial climatic warming and wetting. The
568 gradual establishment of deciduous woody vegetation was not sufficient to
569 stabilize the landscape or prevent large-scale mobilization of the silt, plus the
570 formation of lakes, gullies, and flooded drainages. Furthermore, it may have
571 enhanced fire-related thermokarst initiation. The changes recorded in the
572 sediments and surface topography of the marginal upland serve as a reminder
573 that significant shifts in warmth, moisture and disturbance regime can lead to
574 dramatic alterations of the landscape and rapid shifts in the rate and nature of
575 geomorphic processes (i.e., a regime shift). The dynamic changes in the
576 marginal upland appear to have “switched off” quite early in the Holocene,

577 representing a second regime shift. Though partial drainage of lakes evidently
578 still occurs, the current landscape largely reflects past, not current, geomorphic
579 activity. The slow-down in permafrost degradation may be partly due to previous
580 depletion of most near-surface massive ice, plus the spread of dense, boreal
581 forest in the mid Holocene and associated changes in surface shading,
582 enhanced insulation by thickening organic layers, and decrease in the active
583 layer.

584 In contrast, in other regions, such as the northern Seward Peninsula and
585 Arctic Coastal Plain of northern Alaska, thermokarst has evidently been active
586 throughout the Holocene (Hopkins and Kidd, 1988; Hinkel et al., 2003; Jones et
587 al., 2012; Wetterich et al., 2012), and yedoma deposits have in some places
588 been reduced by repetitive lake formation and drainage to a base level tens of
589 meters lower than the original upland surface (Grosse et al., 2007; Veremeeva
590 and Gubin, 2009, Morgenstern et al., 2011). Lakes in the Arctic tundra lowlands
591 dominated by ice-rich surface sediments frequently drain completely due to rapid
592 and deep incision of drainage gullies (Marsh and Neumann, 2011, Jones et al.,
593 2011; Grosse et al., 2013; Jones and Arp, 2015). These landscapes strongly
594 reflect recent and contemporary thermokarst processes, as well a history of lake
595 formation and drainage over the Holocene. Furthermore, the vegetation cover is
596 tundra, not forest, the regional moisture balance is positive, and field evidence
597 suggests a greater volume of ground ice present in the yedoma. The latter two
598 features likely increase the probability of thermokarst lake dynamism compared
599 with the Yukon Flats.

Looking to the future, the dense forest cover in the Yukon Flats will likely confer a strong inertia against expected climate warming. If future warming is associated with enhanced moisture, then lakes could conceivably overflow, but if the precipitation and evaporation-driven moisture deficit persists in the study region drainage is unlikely. However, with strong arctic warming comes the possibility of increased frequency of burning (Kasischke et al., 2010; Kelly et al., 2013), which itself may accelerate permafrost loss over time, via destruction of the insulating organic layer (Brown et al., 2015). In turn, this may lead to local remobilization of the silt and/or the opening up of near-surface drainage pathways and loss of water locally from lakes and ponds, as has apparently happened in the Yukon Flats lowland (Chen et al., 2014, Minsley et al., 2012) and on the southern Seward Peninsula (Yoshikawa & Hinzman, 2003).

Knowledge of the evolution of thermokarst-lake landscapes and the key underlying processes provides a better basis for projecting possible future scenarios. The differences between the yedoma and thermokarst lakes of, for example, the northern Seward Peninsula and the Yukon basin emphasize that not all Holocene thermokarst-lake landscapes are similar, and neither are the pathways by which they developed. While the nature of a given thermokarst regime is a reflection of current environmental conditions, its dependence on previously determined conditions, particularly topography and the nature of ground-ice, and vegetation and disturbance regime is also important. Furthermore, not only rates but directions of developmental trajectories can change. This heterogeneity has consequences for landscape resilience in the

face of major climate change. Models of how such landscapes behave now or will do in the future (e.g., van Huissteden et al., 2011) should, therefore, acknowledge specific regional conditions, and up-scaled estimates of change should be applied with caution.

Acknowledgements

The late David M. Hopkins inspired our initial study and provided many insights into the thermokarst lakes and landscape of the Yukon Flats marginal upland. Bob Anderson, Pat Anderson, Nancy Bigelow, Les Cwynar, Peter Dunwiddie, Bruce Finney, Richard Grey, Chris Panks, and Dave Yamaguchi all helped with fieldwork that contributed to this paper. The LiDAR images were supplied by the US Geological Survey. Aquatic shells were identified by Nora Foster. The following grants supported this work: NSF-DPP 8303734 to ME and ERC #338335 to GG. We thank Lesleigh Anderson and three anonymous reviewers for helpful suggestions that improved the manuscript. Any use of trade, product, or firm names is for descriptive purposes only and does not imply endorsement by the U.S. Government.

References

Abbott, M.B., Finney, B.P., Edwards, M.E., Kelts, K.R., 2000. Lake-level reconstructions and paleohydrology of Birch Lake, central Alaska, based on

644 seismic reflection profiles and core transects. Quaternary Research 53,154-
645 166.
646 Anderson, P.M., Edwards, M.E., Brubaker, L.B., 2004. Results and paleoclimate
647 implications of 35 years of paleoecological research in Alaska. In: Gillespie,
648 A.E., Porter, S.C., Atwater, B.F. (Eds.), The Quaternary Period in the United
649 States. Developments in Quaternary Science. Elsevier, New York, pp. 427-
650 440.
651 Anderson, L., Birks, J., Rover, J., Guldager, N., 2013. Controls on recent Alaskan
652 lake changes identified from water isotopes and remote sensing. Geophysical
653 Research Letters 40, 3413–3418.
654 Arp, C.D., Jones, B.M., 2008. Geography of Alaska Lake Districts: Identification,
655 Description, and Analysis of Lake-Rich Regions of a Diverse and Dynamic
656 State. USGS Scientific Investigations Report 2008-5215.
657 Arp, C.D., Jones, B.M., Urban, F.E., Grosse, G., 2011. Hydrogeomorphic
658 processes of thermokarst lakes with grounded-ice and floating-ice regimes on
659 the Arctic coastal plain, Alaska. Hydrological Processes 25, 2422-2438.
660 Barber, V.A., Finney, B.P., 2000. Late Quaternary paleoclimatic reconstructions
661 for interior Alaska based on paleolake-level data and hydrologic models.
662 Journal of Paleolimnology 24, 29-41.
663 Bartlein, P.J., Anderson, P.M., Edwards, M.E., McDowell, P.F., 1991. A
664 framework for interpreting paleoclimatic variations in eastern Beringia.
665 Quaternary International 10, 73-83.

666 Bartlein, P.J., Hostetler, S.W., Alder, J.R., 2014. Paleoclimate. In: Ohring, G.
667 (Ed.), Climate Change in North America. Regional Climate Studies. Springer,
668 New York, pp. 1–51.
669 Bastviken, D., 2004. Methane emissions from lakes: Dependence of lake
670 characteristics, two regional assessments, and a global estimate, Global
671 Biogeochemical Cycles 18, GB4009, DOI:10.1029/2004GB002238.
672 Bigelow, N.H., Edwards, M.E., Elias, S.E., Hamilton, T.D., Schweger, C.E., 2014.
673 Tundra and boreal forest of interior Alaska during terminal MIS 6 and MIS 5e.
674 Vegetation History and Archaeobotany 23,177–193.
675 Bockheim, J.G., Hinkel, K.M., Eisner, W.R., Dai, X.Y., 2004. Carbon pools and
676 accumulation rates in an age-series of soils in drained thaw-lake basins, Arctic
677 Alaska. Soil Science Society of America Journal 68, 697-704.
678 Brown, D.R.N., Jorgenson, M.T., Douglas, T.A., Romanovsky, V.E., Kielland, K.,
679 Hiemstra, C., Euskirchen, E.S., Ruesss, R.W., 2015. Interactions of fire and
680 climate exacerbate permafrost degradation in Alaskan lowland forests. Journal
681 of Geophysical Research – Biogeosciences 120, 1619–1637, DOI
682 10.1002/2015JG003033
683 Burn, C.R., 1997. Cryostratigraphy, paleogeography, and climate change during
684 the early Holocene warm interval, western Arctic coast, Canada. Canadian
685 Journal of Earth Sciences 34, 912-925.
686 Burn, C.R., 2002. Tundra lakes and permafrost, Richards Island, western Arctic
687 coast, Canada. Canadian Journal of Earth Sciences 39, 1281-1298.

688 Burn, C.R., Smith, M.W., 1990. Development of thermokarst lakes during the
689 Holocene at sites near Mayo, Yukon Territory. Permafrost and Periglacial
690 Processes 1, 161-176.
691 Chen, M., Rowland, J.C., Wilson, C.J., Altmann, G.L., Brumby, S.P., 2014.
692 Temporal and spatial pattern of thermokarst lake area changes at Yukon Flats,
693 Alaska. Hydrological Processes 28, 837–852.
694 Edwards, M.E. and Hopkins, D.M. 1988. Deep thermokarst lakes in the southern
695 Yukon Flats, Alaska. Abstracts, 39th Arctic Science Conference, American
696 Association for the Advancement of Science, Arctic Division, Fairbanks, p 207.
697 Edwards, M.E., McDowell, P.F., 1991. Interglacial deposits at Birch Creek,
698 northeast interior Alaska. Quaternary Research 35, 41-52.
699 Edwards, M.E., Hopkins, D.M., Mann, D.H., 1995. Long-term effects of
700 thermokarst on landscape development in Alaska and Siberia. Program and
701 Abstracts, 46th Arctic Science Conference, American Association for the
702 Advancement of Science, Arctic Division, Fairbanks, p 24.
703 Faegri, K., Iversen, J., 1989. Textbook of Pollen Analysis. 4th Edition. Wiley,
704 London, 328 pp.
705 Farquharson, L., Walter Anthony, K.M., Bigelow, N.H., Edwards, M.E., Grosse
706 G., Accepted. Facies analysis of yedoma thermokarst lakes on the northern
707 Seward Peninsula, Alaska. Sedimentary Geology.
708 Fedorov, A.N., Gavriliev, P.P., Konstantinov, P.Y., Hiyama, T., Iijima, Y.,
709 Iwahana, G., 2014. Estimating the water balance of a thermokarst lake in the
710 middle of the Lena River basin, eastern Siberia. Ecohydrology 7, 188–196.

711 French, H.M., 2007. The Periglacial Environment, 3rd Edition. Wiley, Chichester,
712 478 pp.
713 Grosse, G., Schirrmeister, L., Siegert, C., Kunitsky, V.V., Slagoda, E.A., Andreev,
714 A.A., Dereviagyn, A.Y., 2007. Geological and geomorphological evolution of a
715 sedimentary periglacial landscape in Northeast Siberia during the Late
716 Quaternary. Geomorphology 86, 25-51.
717 Grosse, G., Jones, B., Arp, C., 2013. Thermokarst Lakes, Drainage, and Drained
718 Basins. In: Shroder, J.F. (Ed.), Treatise on Geomorphology, Vol. 8 Academic
719 Press, San Diego, pp. 325-353.
720 Heglund, P.J., Jones, J.R., 2003. Limnology of shallow lakes in the Yukon Flats
721 National Wildlife Refuge, Interior Alaska. Lake and Reservoir Management 19,
722 133-140.
723 Hinkel, K.M., Eisner, W.R., Bockheim, J.G., Nelson, F.E., Peterson, K.M., Dai,
724 X.Y., 2003. Spatial extent, age, and carbon stocks in drained thaw lake basins
725 on the Barrow Peninsula, Alaska. Arctic Antarctic and Alpine Research 35,
726 291-300.
727 Hinkel, K.M., Frohn, R.C., Nelson, F.E., Eisner, W.R., Beck, R.A., 2005.
728 Morphometric and spatial analysis of thaw lakes and drained thaw lake basins
729 in the western Arctic Coastal Plain, Alaska. Permafrost and Periglacial
730 Processes 16, 327-341.
731 Hinkel, K.M., Jones, B.M., Eisner, W.R., Cuomo, C.J., Beck, R.A., Frohn, R.,
732 2007. Methods to assess natural and anthropogenic thaw lake drainage on the

western arctic coastal plain of northern Alaska. Journal of Geophysical Research 112, F02S16, DOI:10.1029/2006JF000584.

Hinkel, K.M., Sheng, Y., Lenters, J.D., Lyons, E.A., Beck, R.A., Eisner, W.R., Wang, J.D., 2012. Thermokarst Lakes on the Arctic Coastal Plain of Alaska: Geomorphic Controls on Bathymetry. Permafrost and Periglacial Processes 23, 218-230.

Hopkins, D.M., Kidd, J.G., 1988. Thaw-lake sediments and sedimentary environments. Fifth International Permafrost Conference Proceedings Vol. 1, Trondheim, Norway, pp. 790-795.

Jepsen, S.M., Voss, C.I., Walvoord, M.A., Minsley, B.J., Rover J., 2013. Linkages between lake shrinkage/expansion and sublacustrine permafrost distribution determined from remote sensing of interior Alaska, USA. Geophysical Research Letters 40, 882–887.

Jones, B.M., Arp, C.D., 2015. Observing a catastrophic thermokarst lake drainage in northern Alaska. Permafrost and Periglacial Processes 26, 119-128.

Jones, B.M., Grosse, G., Arp, C.D., Jones, M.C., Walter Anthony, K.M., Romanovsky. V.E., 2011. Modern thermokarst lake dynamics in the continuous permafrost zone, northern Seward Peninsula, Alaska. Journal of Geophysical Research – Biogeosciences 116, G00M03, DOI:10.1029/2011JG001666.

Jones, M.C., Grosse, G., Jones, B.M., Walter Anthony, K.M., 2012. Peat accumulation in a thermokarst-affected landscape in continuous ice-rich

permafrost, Seward Peninsula, Alaska. Journal of Geophysical Research – Biogeosciences 117, G00M07, DOI:10.1029/2011JG001766.

Jorgenson, M.T., Shur, Y., 2007. Evolution of lakes and basins in northern Alaska and discussion of the thaw lake cycle. Journal of Geophysical Research – Earth Surface 112, Issue: F2, Article Number: F02S17

Jorgenson, M.T., Romanovsky, V., Harden, J., Shur, Y., O'Donnell, J., Schuur, E.A.G., Kanevskiy, M., Marchenko, S., 2010. Resilience and vulnerability of permafrost to climate change. Canadian Journal of Forest Research 40, 1219-1236.

Kanevskiy, M., Shur, Y., Fortier, D., Jorgenson, M.T., Stephani, E., 2011. Cryostratigraphy of late Pleistocene syngenetic permafrost (yedoma) in northern Alaska, Itkillik River exposure. Quaternary Research 75, 584-596.

Kasischke, E.S., Verbyla, D.L., Rupp, T.S., McGuire, A.D., Murphy, K.A., Jandt, R., Barnes, J.L., Hoy, E.E., Duffy, P.A., Calef, M., Turetsky, M.R., 2010. Alaska's changing fire regime – Implications for the vulnerability of its boreal forests. Canadian Journal of Forest Research 40, 1313–1324.

Katamura, F., Fukuda, M., Bosikov, N.P., Desyatkin, R.V., 2009. Charcoal records from thermokarst deposits in central Yakutia, eastern Siberia: Implications for forest fire history and thermokarst development, Quaternary Research, 71, 36-40.

Kaufman, D., Ager, T., Anderson, N., Anderson, P., Andrews, J., Bartlein, P., Brubaker, L., Coats, L., Cwynar, L., Duvall, M., Dyke, A., Edwards, M., Eisner, W., Gajewski, K., Geirsdóttir, A., Hu, F., Jennings, A., Kaplan, Kerwin, M.,

779 Lozhkin, A., MacDonald, G., Miller, G., Mock, C., Oswald, W., Otto-Bliesner,
780 B., Porinchu, D., Rühland, K., Smol, J., Steig, E., Wolfe, B., 2004. Holocene
781 thermal maximum in the western arctic (0–180°W). Quaternary Science
782 Reviews 23, 529–560.
783 Kelly R., Chipman M.L., Higuera P.E., Stefanova, I., Brubaker, L.B., Hu, F-S.,
784 2013. Recent burning of boreal forests exceeds fire regime limits of the past
785 10,000 years. PNAS 110, 13055–13060.
786 Kessler, M.A., Plug, L.J., Walter Anthony, K.M., 2012. Simulating the decadal- to
787 millennial-scale dynamics of morphology and sequestered carbon mobilization
788 of two thermokarst lakes in NW Alaska. Journal of Geophysical Research –
789 Biogeosciences 117, G00M06. DOI:10.1029/2011jg001796.
790 Lantz, T. C., Turner, K. W., 2015. Changes in lake area in response to
791 thermokarst processes and climate in Old Crow Flats, Yukon. Journal of
792 Geophysical Research – Biogeosciences 120, 513-524.
793 Lauriol, B., Lacelle, D., Labrecque, S., Duguay, C.R., Telka, A., 2009. Holocene
794 Evolution of Lakes in the Bluefish Basin, Northern Yukon, Canada. Arctic 62,
795 212-224.
796 Lenz, J., Grosse, G., Jones, B., Walter Anthony, K., Bobrov, A., Wulf, S,
797 Wetterich, S., 2015. Mid-Wisconsin to Holocene permafrost and landscape
798 dynamics on the northern Seward Peninsula, Northwest Alaska, based on a
799 drained lake basin core. Permafrost and Periglacial Processes. Paper in
800 press.

801 Mackay, J.R., 1988. Catastrophic lake drainage, Tuktoyaktuk Peninsula area,
802 District of Mackenzie. In: Current Research, Part D. Geological Survey of
803 Canada, pp. 83–9.
804 Marsh, P., Neumann, N., 2001. Processes controlling the rapid drainage of two
805 ice-rich permafrost-dammed lakes in NW Canada. Hydrological Processes 15,
806 3433–3446.
807 Marsh, P., Russell, M., Pohl, S., Haywood, H. and Onclin, C., 2009. Changes in
808 thaw lake drainage in the Western Canadian Arctic from 1950 to 2000.
809 Hydrological Processes 23, 145–158.
810 McDowell, P.F., Edwards, M.E., 2001. Evidence of Quaternary climatic variations
811 in a sequence of loess and related deposits at Birch Creek, Alaska:
812 implications for the stage 5 climatic chronology. Quaternary Science Reviews
813 20, 63-76.
814 Minsley, B.J., Abraham, J.D., Smith, B.D., Cannia, J.C., Voss, C.I., Jorgenson,
815 M.T., Walvoord, M.A., Wylie, B.K., Anderson, L., Ball, L.B., Deszcz-Pan, M.,
816 Wellman, T.P., Ager, T.A., 2012. Airborne electromagnetic imaging of
817 discontinuous permafrost, Geophysical Research Letters 39, L02503,
818 DOI:10.1029/2011GL050079
819 Morgenstern, A., Grosse, G., Gunther, F., Federova, I., Schirrmeister, L., 2011.
820 Spatial analysis of thermokarst lakes and basins in Yedoma landscapes of the
821 Lena Delta. The Cryosphere 5, 849-867.
822 Murton, J.B., 1996. Thermokarst-lake-basin sediments, Tuktoyaktuk Coastlands,
823 western arctic Canada. Sedimentology 43, 737-760.

824 Murton, J.B., Goslar, T., Edwards, M.E., Bateman, M.D., Danilov, P.P., Savvinov,
825 G.N., Gubin, S.V., Ghaleb, B., Haile, J., Kanevskiy, M., Lozhkin, A.V.,
826 Lupachev, A.V., Murton, D.K., Shur, Y., Tikhonov, A., Vasil'chuk, A.C.,
827 Vasil'chuk, Y.K., Wolfe, S.A., 2015. Aeolian deposition, chronology and
828 palaeoenvironments of Late Pleistocene yedoma silts (Ice Complex) at
829 Duvanny Yar, NE Siberia. Permafrost and Periglacial Processes 26, 208-288.
830 Paltan, H., Dash, J., Edwards, M., 2015. A refined mapping of Arctic lakes using
831 Landsat imagery. Journal of Remote Sensing 36, 5970-5982.
832 Rampton, V., 1971. Late Quaternary vegetational and climatic history of the Snag
833 Klutlan area, southwestern Yukon Territory, Canada. Geological Society of
834 America Bulletin 82, 959-978.
835 Reimer, P.J., Bard, E., Bayliss, A., Beck, J.W., Blackwell, P.G., Bronk Ramsey,
836 C., Buck, C.E., Cheng, H., Edwards, R.L., Friedrich, M., Grootes, P.M.,
837 Guilderson, T.P., Haflidason, H., Hajdas, I., Hatté, C., Heaton, T.J., Hoffman,
838 D.L., Hogg, A.G., Hughen, K.A., Kaiser, K.F., Kromer, B., Manning, S.W., Niu,
839 M., Reimer, R.W., Richards, D.A., Scott, E.M., Southon, J.R., Staff, R.A.,
840 Turney, C.A., van der Plicht, J., 2013. INTCAL13 and marine13 radiocarbon
841 age calibration curves 0–50,000 Years Cal BP. Radiocarbon 55, 1869–1887.
842 Riordan, B., Verbyla, D., McGuire, A.D. 2006. Shrinking ponds in subarctic
843 Alaska based on 1950–2002 remotely sensed images. Journal of Geophysical
844 Research, 111, G04002, DOI:10.1029/2005JG000150.

Roach, J., Griffith, B., Verbyla, D. Jones, J., 2011. Mechanisms influencing changes in lake area in Alaskan boreal forest. Global Change Biology 17, 2567–2583.

Robinson, S., Beaudoin, A.B., Froese, D.G., Doubt, J., Clague, J.J., 2007. Plant macrofossils associated with an early Holocene beaver dam in interior Alaska. Arctic 60, 430-438.

Schirrmeister, L., Froese, D., Tumskoy, V., Grosse, G., Wetterich, S., 2013. Yedoma. Encyclopedia of Quaternary Science, Vol. 3, 542–552.

Sellmann, P.V., Brown, J., Lewellen, R.I., McKim, H., Merry, C., 1975. The classification and geomorphic implications of thaw lakes on the Arctic Coastal Plain, Alaska. Research Report 344, Cold Regions Research and Engineering Laboratory, Hanover, New Hampshire, 21 pp.

Smith, L.C., Sheng, Y., MacDonald, G.M., Hinzman, L.D., 2005. Disappearing Arctic lakes. Science 308, 1429–1429.

van Huissteden, J., Berrittella, C., Parmentier, F.J.W., Mi, Y., Maximov, T.C., Dolman, A.J., 2011. Methane emissions from permafrost thaw lakes limited by drainage. Nature Climate Change 1, 119-123.

Veremeeva, A., Gubin, S., 2009. Modern tundra landscapes of the Kolyma Lowland and their evolution in the Holocene. Permafrost and Periglacial Processes 20, 399–406.

Vermaire, J.C., 2005. Late-Quaternary vegetation histories from Antifreeze and Eikland Ponds, southwestern Yukon Territory, Canada. M.Sc. Thesis. The University of New Brunswick.

868 Viereck, L.A., 1970. Forest succession and soil development adjacent to the
869 Chena River in interior Alaska. Arctic and Alpine Research 2, 1-26.
870 Walter, K.M., Zimov, S.A., Chanton, J.P., D., V., Chapin III, F. S., 2006. Methane
871 bubbling from Siberian thaw lakes as a positive feedback to climate warming.
872 Nature 443, 71–5.
873 Walter, K.M., Edwards, M.E., Grosse, G., Zimov, S.A., Chapin, F.S. III., 2007a.
874 Thermokarst lakes as a source of atmospheric CH_4 during the last
875 deglaciation. Science 318, 633-636.
876 Walter, K.M., Smith, L.C., Chapin, F.S., 2007b. Methane bubbling from northern
877 lakes: present and future contributions to the global methane budget.
878 Philosophical Transactions, Series A, Mathematical, Physical, and
879 Engineering Sciences, 365, 1657–76.
880 Walter Anthony, K.M., Zimov, S., Grosse, G., Jones, M.C., Anthony, P.M.,
881 Chapin, F.S., Finlay, J.C., Mack, M.C., Davydov, S., Frenzel, P. Frolking, S.,
882 2014. A shift of thermokarst lakes from carbon sources to sinks during the
883 Holocene epoch. Nature 511, 452–456.
884 Walvoord, M.A., Voss, C.I., Wellman, T.P., 2012. Influence of permafrost
885 distribution on groundwater flow in the context of climate-driven permafrost
886 thaw: Example from Yukon Flats Basin, Alaska, United States. Water
887 Resources Research 48, W07524, DOI: 10.1029/2011WR011595.
888 West, J.J. and Plug, L.J., 2008. Time-dependent morphology of thaw lakes and
889 taliks in deep and shallow ground ice. Journal of Geophysical Research 113,
890 F01009, DOI: 10.1029/2006JF000696

Wetterich, S., Grosse, G., Schirrmeister, L., Andreev, A.A., Bobrov, A.A., Kienast, F., Bigelow, N.H., Edwards, M.E., 2012. Late Quaternary environmental and landscape dynamics revealed by a pingo sequence on the northern Seward Peninsula, Alaska. Quaternary Science Reviews 39, 26–44.

Williams, J.R., 1962. A geologic reconnaissance, Yukon Flats district, Alaska. U.S. Geological Survey Bulletin 111-H, Washington, DC, pp. 290-311.

Williams, J.R., Yeend, W.E., 1979. Deep thaw lake basins in the inner Arctic Coastal Plain, Alaska. In Johnson, K.M., & Williams, J.R., (Eds.).US Geological Survey in Alaska: Accomplishments during 1978. Washington, D.C.

Wright, H.E., 1967. A square rod piston sampler for lake sediments. Journal of Sedimentary Petrology 37, 975–976.

Yoshikawa, K., Hinzman, L.D., 2003. Shrinking thermokarst ponds and groundwater dynamics in discontinuous permafrost near Council, Alaska. Permafrost & Periglacial Processes 14, 151–160.

Zimov, S.A., Voropaev, Y.V., Semiletov, I.P., Davidov, S.P., Prosiannikov, S.F., Chapin, F.S., Chapin, M.C., Trumbore, S., Tyler, S., 1997. North Siberian lakes: A methane source fueled by Pleistocene carbon. Science 277, 800-802.

Zulueta, R.C., Oechel, W.C., Loescher, H.W. Lawrence, W.T., Paw U, K.T., 2011. Aircraft-derived regional-scale CO2 fluxes from vegetated drained thaw-lake basins and interstitial tundra on the Arctic Coastal Plain of Alaska. Global Change Biology 17, 2781-2802.

Figure Captions

Fig. 1. Map of the study area. The southern marginal upland is enclosed by the dashed black line. SOT: Sands of Time Lake; 6LL: Six-Loon Lake; D2: Dune Two Lake; BC-1: Birch Creek section (McDowell and Edwards, 2001). Major rivers originating in the Yukon-Tanana uplands, which expose the sediments of the marginal upland in river-cut bluffs, can be seen as low-elevation corridors cutting through the marginal upland. Beaver Creek (see Fig. 4) lies just west of 6LL. On location map of Alaska, NSP indicates the northern Seward Peninsula and ACP the Arctic coastal plain.

Fig. 2. Two terrain-corrected Landsat 7 ETM+ false color images (band combination: 7, 4, 2) showing detail of the marginal upland landscape. Left: the west end of study area. SOT: Sands of Time Lake (a type I swale lake). Right: detail of central portion showing locations of Six-Loon (6LL) and Dune Two (D2) lakes and recent fires. East Lake (see Fig. 6) lies directly east of 6LL. Six-Loon and adjacent lakes are perched (type II) lakes. D2 forms part of a system of drainage (type III) lakes. Pink coloration represents areas that have burned since the 1980s. Source: Landsat Geocover Project: http://glcf.umd.edu/research/portal/geocover/ortho.shtml

Fig. 3. A 1980 false color aerial photograph showing the Six-Loon Lake (6LL) area. Pale strips at lake margins are sparsely vegetated silt bluffs (B). Low, sub-parallel ridges (corrugations; C) and apparent drainage channels (D) are also

visible (compare with Fig. 5b). Photo ID: AR5800029298793; Acquisition Date: 05-AUG-80 (Source: USGS Earth Explorer, http://earthexplorer.usgs.gov).

Fig. 4. Bluff ca. 30 m high cut by Beaver Creek showing thaw gully and exposed massive ground ice (arrow). The height scale shown is approximate.

Fig. 5. LiDAR hillshade images of the southern marginal upland acquired in 2009. (a) partially drained lakes, gullies and drainage channels at the edge of the marginal upland. (b) Six-Loon Lake area showing linear corrugations interrupted by lakes (white arrow). It is evident the water level of the largest lake has dropped. Possible lake drainage pathways are indicated by black arrows, with an underfit stream indicated by the left-most arrow. (c) cross section (A-A') showing elevation profile of corrugations and observed lake level far below lip of basin. (d) central area showing widespread corrugations, both parallel and perpendicular to local slopes, and lakes at different elevations that are connected by current or fossil channels; p—perched lake, v—valley lake.

Fig 6. Landsat ETM+ image pairs from (a) 10 August 2012 and (b) 12 July 2013 showing two partial and one complete lake drainage. Blue denotes newly exposed lake bed plus the drainage/sedimentation pathway created during the event, pink shades indicate areas that burned during the summer of 2009, and green shades indicate areas that have not burned since at least the 1950s. The

parallel no-data stripes visible on the left side of each image are a result of the failure of the Landsat ETM+ scan line corrector.

Fig. 7. Core lithologies and abbreviated biostratigraphic records from Sands of Time Lake (a), Six-Loon Lake (b) and Dune Two Lake (c). Y-axis shows depth below sediment surface. X-axis shows pollen frequencies (percent of sum). Horizontal lines in (b) and (c) reflect abrupt lithologic changes. Radiocarbon-dated samples (cal yr BP) are shown on the far left. In (a) LOI is loss on ignition.

Fig. 8. Conceptual model of factors contributing to long-term thermokarst lake and landscape development.

Table 1. Radiocarbon dates for Six-Loon, Dune Two and Sands of Time Lakes, reported as conventional ^{14}C and calibrated ages on 10-cm sections of core (mid-point given). QL-1721 is an extended-count age on *Salix* wood. All other dates are on bulk sediment. Median calibrated ages are based on IntCal 13 (Reimer et al. 2013).

Lab No.	sample mid-point	^{14}C date	error	calibrated age	error
	Six-Loon Lake				
beta 14693	6LL-45	3160	±90	3377	±103
beta 14694	6LL-150	7460	±110	8267	±101
beta 14695	6LL-190	9220	±130	10428	±146
beta 15696	6LL-215	9230	±230	10462	±316
beta 14697	6LL-265	10720	±150	12622	±205
beta 17338	6LL 342	18100	±100	21841	±359
	Dune two Lake				
beta 18524	D2-140	5320	±100	6108	±113
beta 17339	D2-265	9100	±120	10271	± 166
beta 17340	D2-375	11630	±150	13525	± 187

beta 17341	D2-495	10500	±140	12379	± 234
beta 17342	D2-633	10320	±110	12171	± 278
	Sands of Time				
beta 5886	SOT-160	3700	±90	4084	± 132
beta 18523	SOT-250	5130	±70	5867	± 93
beta 4974	SOT-360	7785	±95	8582	± 138
beta 5887	SOT-382	8700	±90	9703	± 147
beta 5888	SOT-420	9060	±80	10225	± 123
beta 4975	SOT-470	10825	±130	12743	± 127
beta 17344	SOT-600	13810	±150	16712	± 238
beta 4590	SOT-710	16590	±440	20050	± 548
beta 17343	SOT-760	21030	±340	25309	± 393
QL-1721	SOT-900	23500	±200	27659	± 153

978

979

980
981

982

983

984

985 FIGURE 1

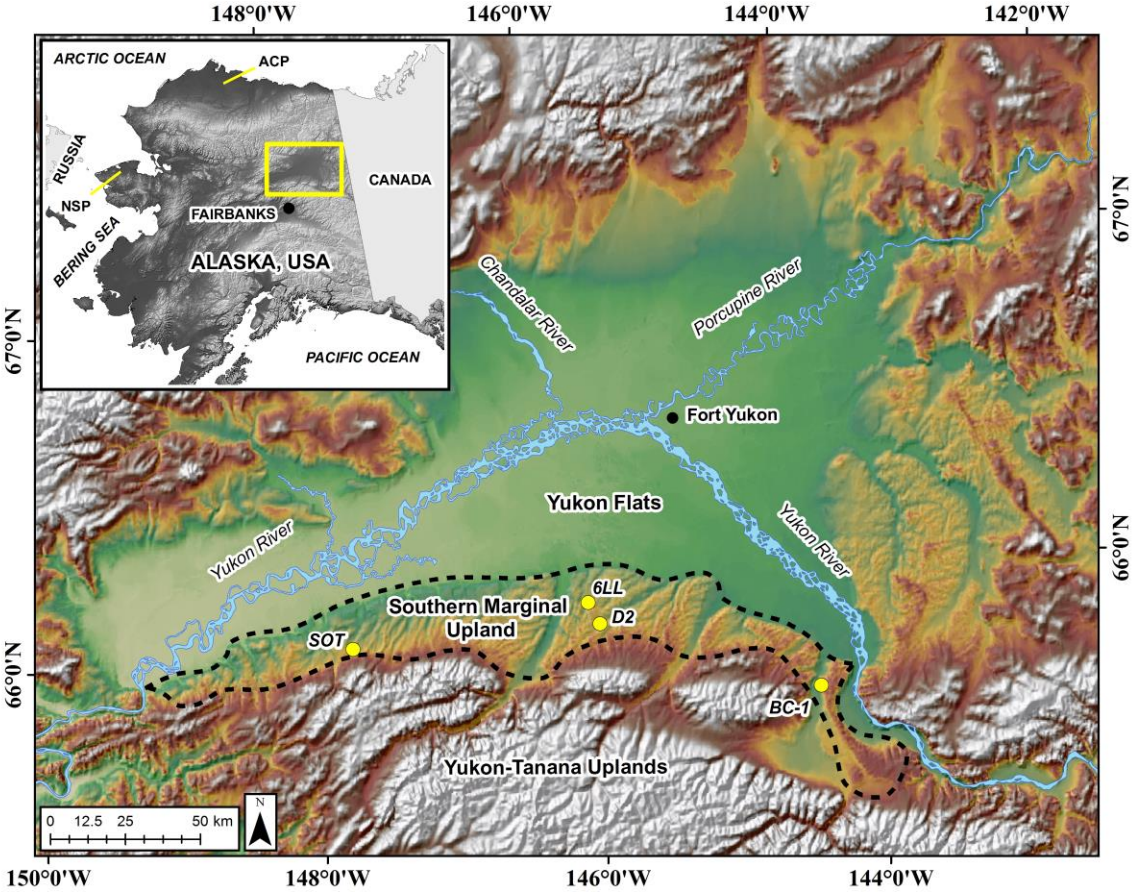

986

987

988 FIGURE 2

989

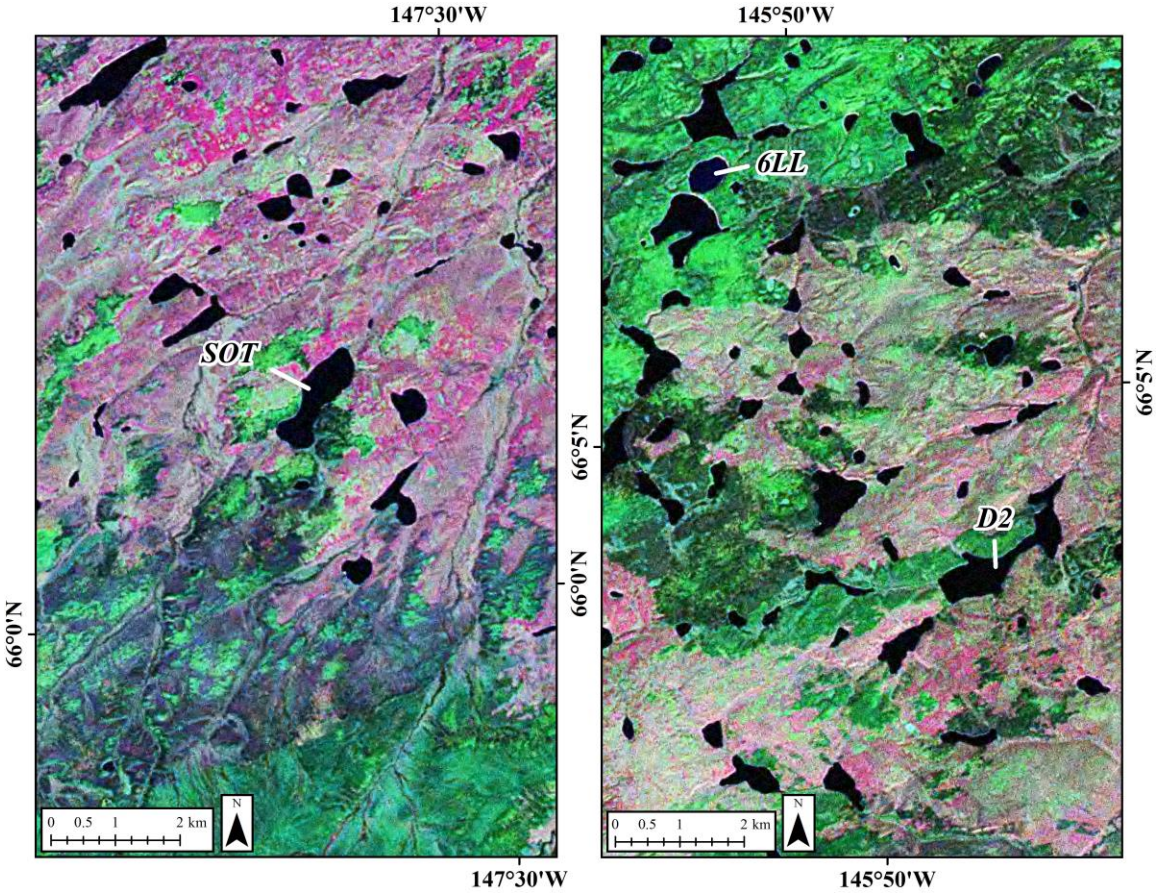

990

991

992 FIGURE 3

993

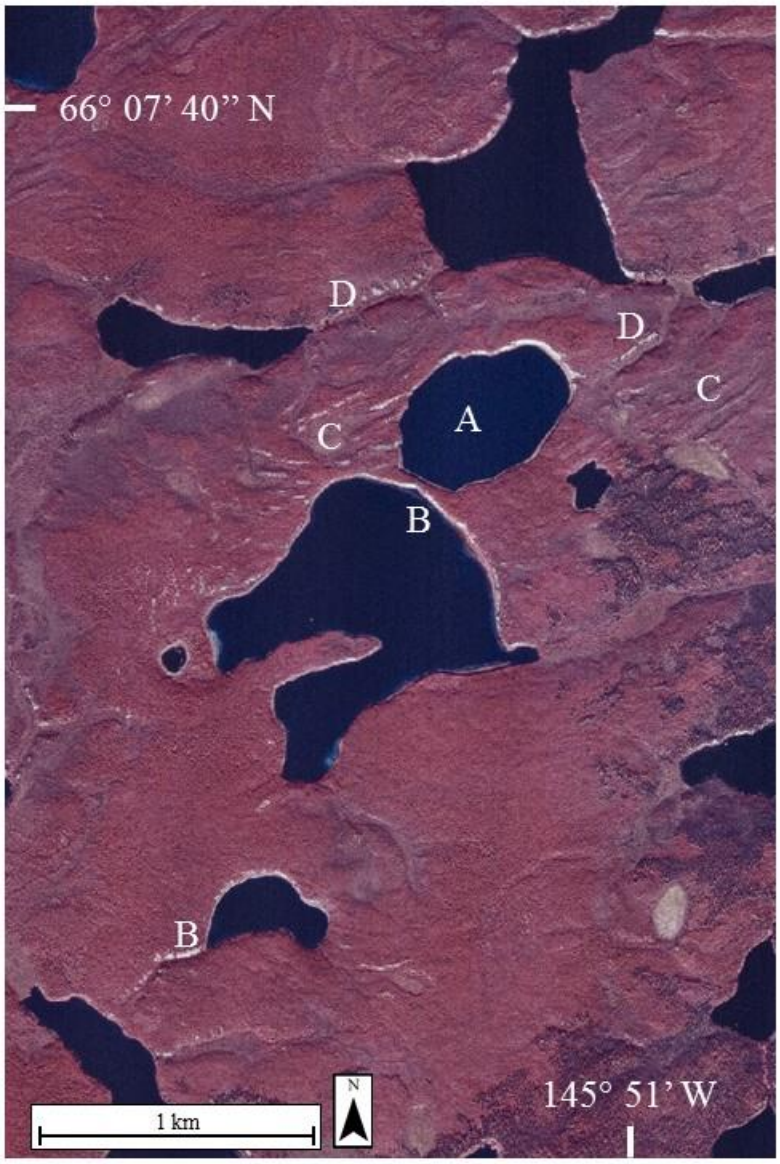

994

995 FIGURE 4

996

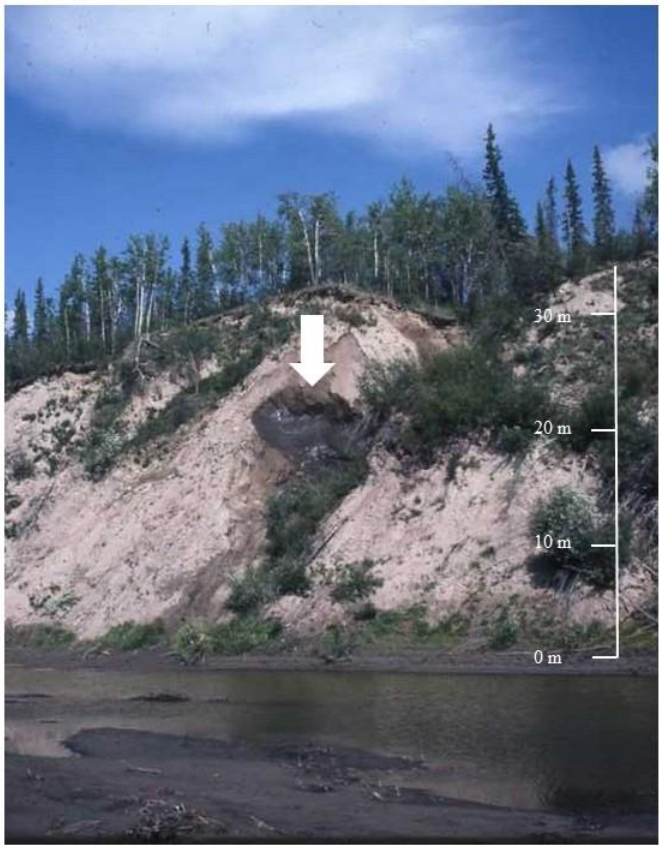

997

998

999 FIGURE 5

1000

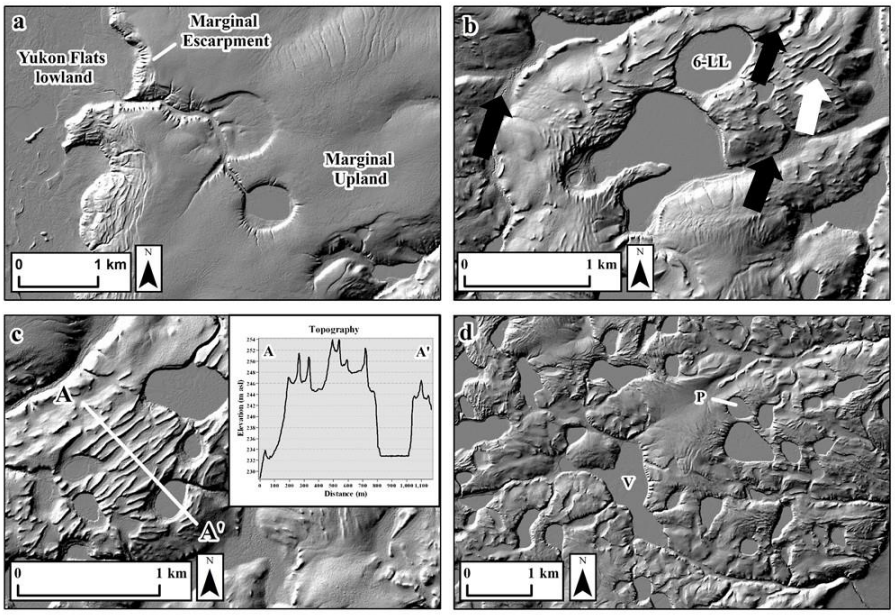

1001

1002

1003

1004 FIGURE 6

1005

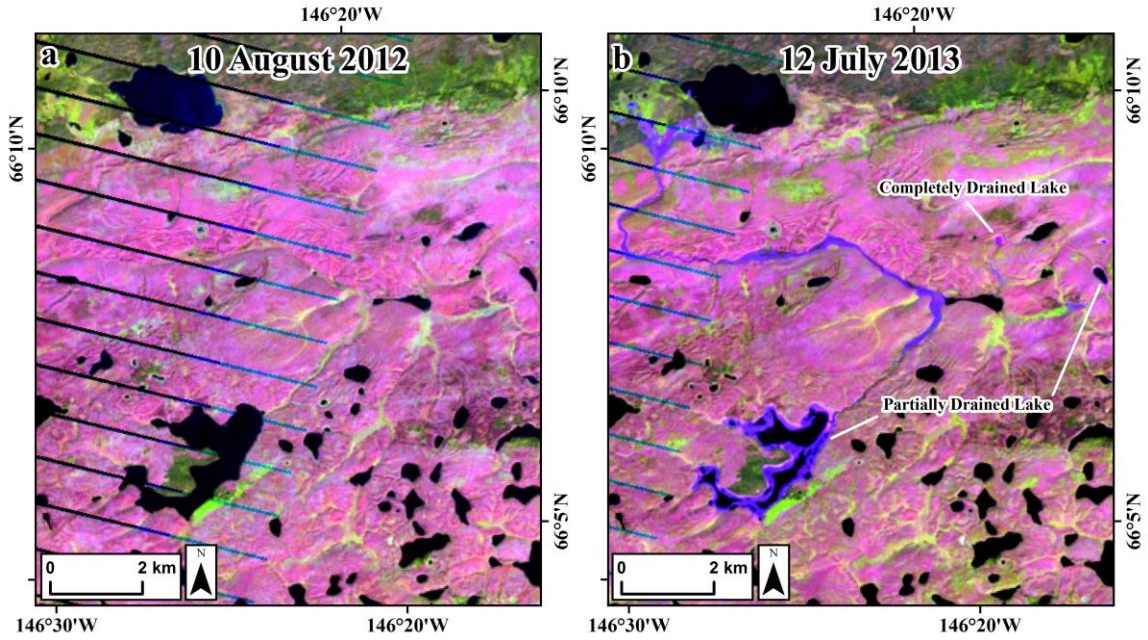

1006

1007

1008

1009 FIGURE 7

1010

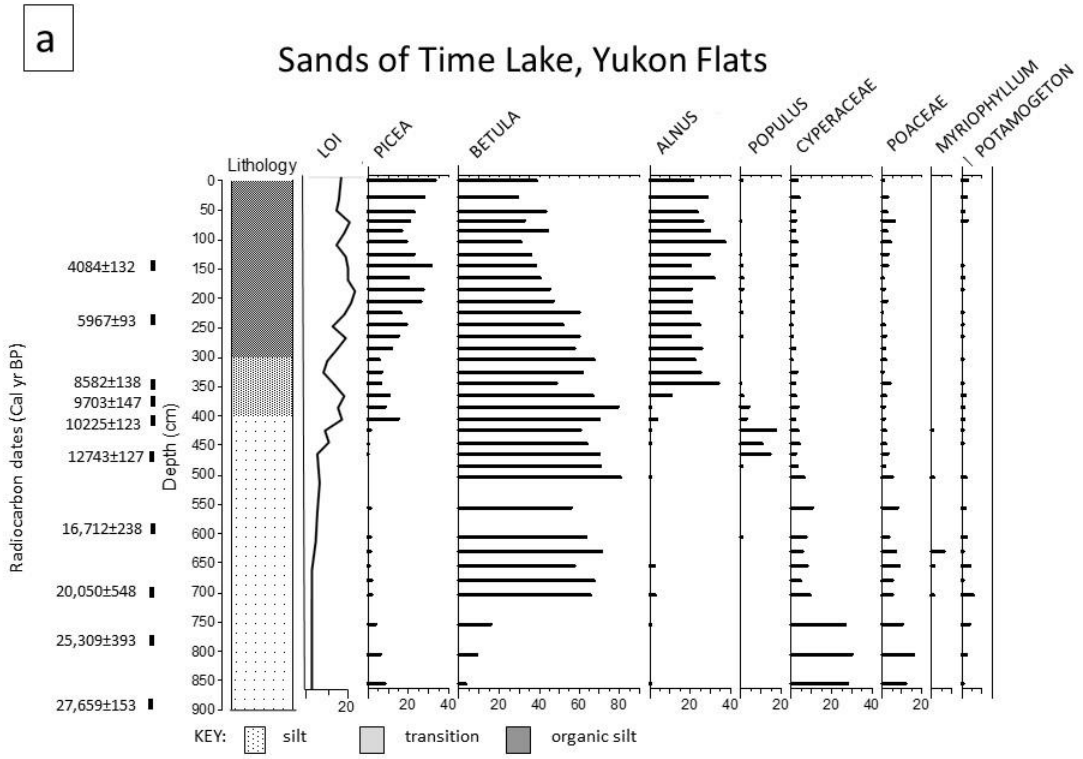

1011

1012

1013

1014

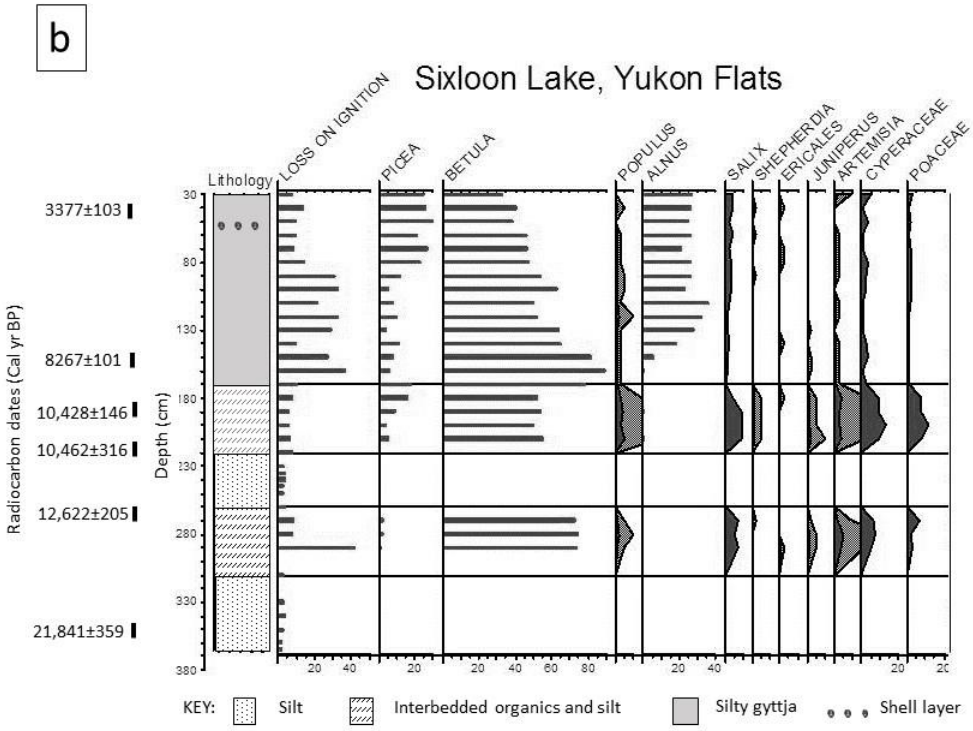

1015

1016

1017

1018

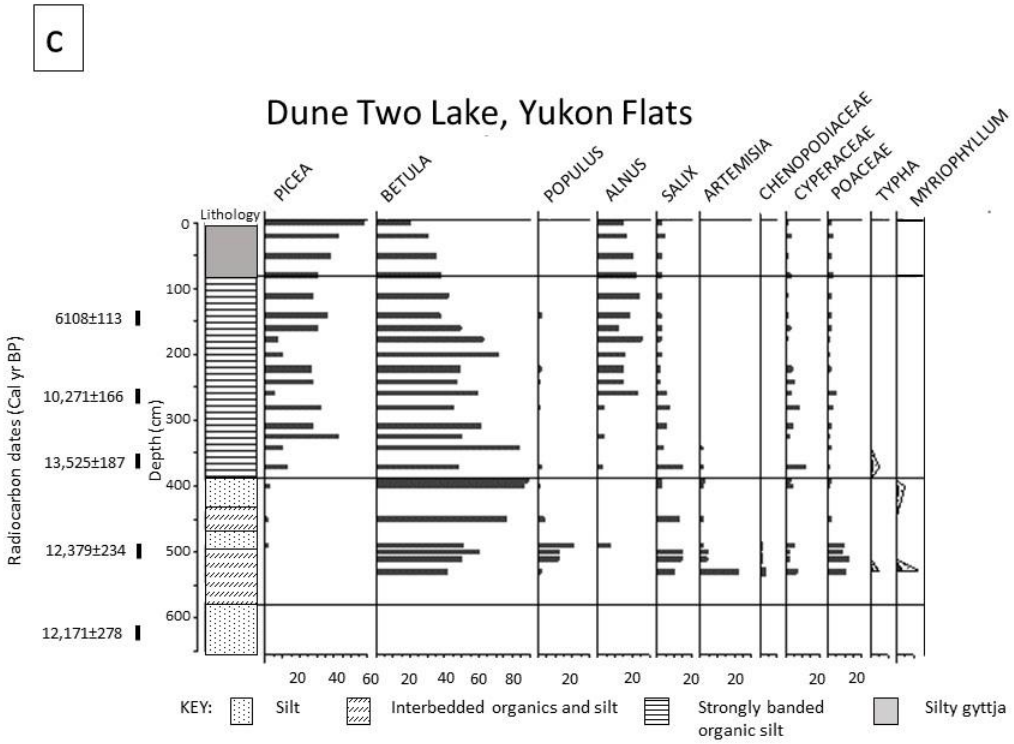

1019

1020

1021

1022 FIGURE 8

1023

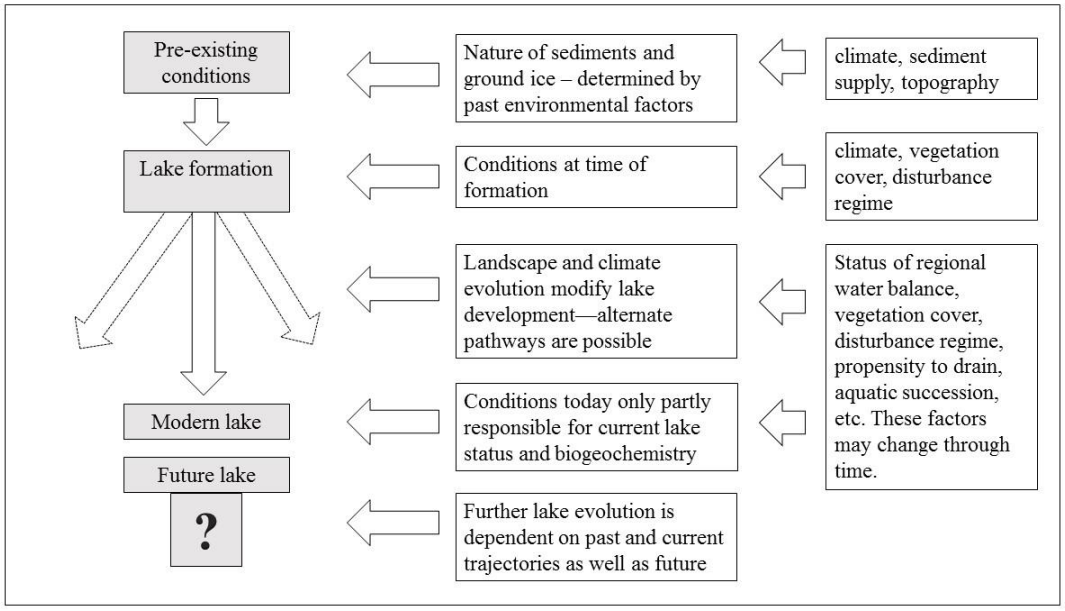

1024

1025

Supplementary data

Notes on representative Yukon Flats southern marginal upland sections, surveyed in July 1983 (PMcD, MEE). In the field, locations were approximated from aerial observation of landing sites linked to map township and range or lat/long.

1. PC-1, Preacher Creek

(65° 8’ N, 145° 18’ W)

0m = top; dimensions below are measurements along sloping tape

0-22m: silty; loess?; very little wood, just a few fine fragments in widely scattered places; abrupt lower boundary

22-24.5m: fluvial sand and silt; alternating beds (0.5-5cm thick) of sand and silty clay loam; tan – dark gray so not very high in organics; few rounded pebbles; beds are contorted and disrupted; a few flame structures intrude upward into beds; some wood oriented parallel to bedding

24.5-33.4m: fluvial deposits; cross-bedded sand layer (thickness not recorded) overlying bedded sand and gravel layers; less wood in this unit, but a little

33.4-68m: sands and gravels (but likely predominantly sands), with woody layer at 35.3-35.47, and scattered organic fragments lower.

Correction to vertical thickness: 22m at 45° = 15m vertical = 22*sine (45°) = 22*.707

Summary: 15m of loess over >30m fluvial sands and gravels

2. BeC-1, Beaver Creek

(South-central part, T14N, R7E, top center of Circle D-5 map)

Trench 1: 0-1m (surface vegetation, soil)

Dimensions below are measurements on sloping tape

1 – 8.4m: silt with peaty and woody debris layers; woody layers with logs at 3.5m, 5m

8.4 – 15m: massive brown-gray silt; no wood or peat noted

Trench 1 stopped at 15m

Correction to vertical thickness for trench 1: angle of tape = 53°; 15*sin(53°) = 12m

Trench 2 is on opposite wall of a gully; starts at 16.5m on tape; measurements below 16.5m are vertical

16.5 – 19.1m: faintly laminated gray-brown silt, same as lower part of trench 1

19.1-19.5m: 0.2m of sand-co silt layers at top, then gravels: trench 2 obscured at 19.5 m and below

In this gully, large ice-wedge melt-out pits at 19m

Summary: 14.5 m retransported silt over fluvial gravels; evidence of ice at about 15m below surface

3. LC-1, Lost Creek

South center, sec. 17, T14N, R2W, Beaver A-2 map

LC-1 is located in the valley wall on west side of Lost Creek valley, not close to the creek

Trench 1 and 2 (at top of exposure)

0-0.4m: soil

0.4-2.85m: massive tan silt, no organics; mottles developed below 1.7m; base of trench 2 at 2.85m

Trench 3 (continues below trenches 1 and 2)

Approx. 2.85-3.9m: massive tan silt, mottled

3.9-4.5m: frozen gray silt; crystalline ice in vertical lens at 4m; bottom of trench 3 at 4.5m

Trench 4 (continues below trench 3)

Approx. 4.5 – 6.5m: frozen silt; few fine organic fragments and wood; this is probably fairly recent slump, did not sample for dating; includes spruce cones, sticks with bark on; bottom of trench at 6.5m

Overall summary: 6.5m of massive tan silt, probably loess; frozen below 3.9m

LC-2, Lost Creek

(approx. 65° 48’ N, 145° 18W)

Exposure on small ridge of silt on valley floor; has Lost Creek at base

vertical exposure

0-1.5m: tan silt with orange bands

1.5-4.3m: tan silt with faint horizontal orange bands and common woody

fragements4.3-5.2m: tan silt with orange bands

5.2m: few small woody fragments

5.2-6.4: tan silt with orange bands, and dark-gray lenses (depositional)

6.4m - 10: fluvial gravels and cobbles

Water level at 10m

Summary of LC-2: 6m of retransported silt over >4m fluvial gravels and cobbles

4. LL-1, Loon Lake (lake adjacent to Six-Loon Lake, Fig. 3)

(66° 6’ N, 145° 52’ W)

Exposure in headwall of slump on NE side of lake

Trench 1: measurements vertical

0-2.2m: tan silt with scattered woody fragments and fragments of freshwater

shell and bone*

2.2 – 4.4mm: massive gray silt, no organics; has some mottles; bottom of trench

at 4.4m

Trench 2: massive gray silt continues 4.4-6m (vertical measurements)

Trench 3: massive gray silt with mottles on surfaces of blocks of silt; continues to

7.3m

Obscured to base of bluff slope, lake water level at 11.3m.

*Recorded shell and bone samples from 1.75-2.1m could be lake deposits.

Lacustrine detritus and sediment at modern lake shore of lake resembles this

shell sample. Observations of geomorphology at site suggest these deposits

could be related to next lake over [i.e., Six Loon Lake], on north side of a narrow

isthmus (See Fig. 3). If these are lake deposits, they are 11m above modern lake level.

Overall summary: at least 7.3m silt; presence of shells suggests this is possibly a lacustrine silt or a high-level beach deposit, possibly related to prior connection between adjacent lakes.